Supporting Information

Dehydration Induced Selective Ion Trapping by Topology Constrained Atomically Thin Graphene-Crown Membranes

Pooja Sahu, Sk. Musharaf Ali*

Bhabha Atomic Research Centre, Mumbai, India 400085

Homi Bhabha National Institute, Mumbai, India 400094

Contents:

Text S1. Details for DFT simulations

Density functional theoretical (DFT) calculation is carried out for the optimization of structures, and thermodynamics of the host (GO-crown ether) and guest species (metal ions) and their complexes using Turbomole suite of program[1]. Calculations were performed with the M06-2X functional[2] using the SVP and TZVP basis set[3, 4]. The aqueous and organic solvent effects in the energetic were included using the COSMO[5] approach. The dielectric constant, ε, of water was taken as 80. The Chimera software was used for the visualization of the various molecular geometries[6] and the calculation of different bond lengths of ligands and their metal ion complexes. The total internal energy (U) of ligand and metal ion–ligand complexes is obtained after adding zero point energy (ZPE) to the electronic energy (E_{el}) [7]. The molecular electrostatic potential (MEPs) of host was determined at the B3LYP/TZP level of theory using ADF suite of package[8, 9].
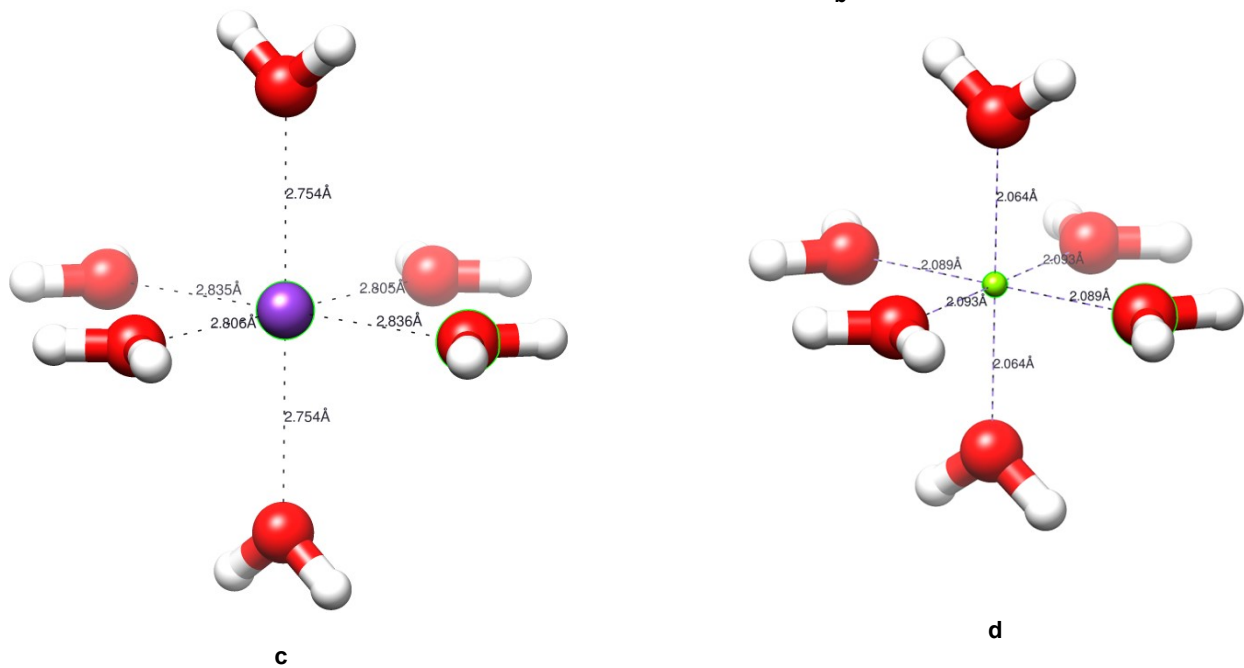
a

b

c

d

Fig. S1: Optimized structure of hydrated metal ions at the M06-2X/SVP level of theory. (a) [Li-$(H_2O)_6]^+$ (b) [Na-$(H_2O)_6]^+$ (c) [K-$(H_2O)_6]^+$ (d) [Mg-$(H_2O)_6]^{2+}$ and (e) [Ca-$(H_2O)_6]^{2+}$.
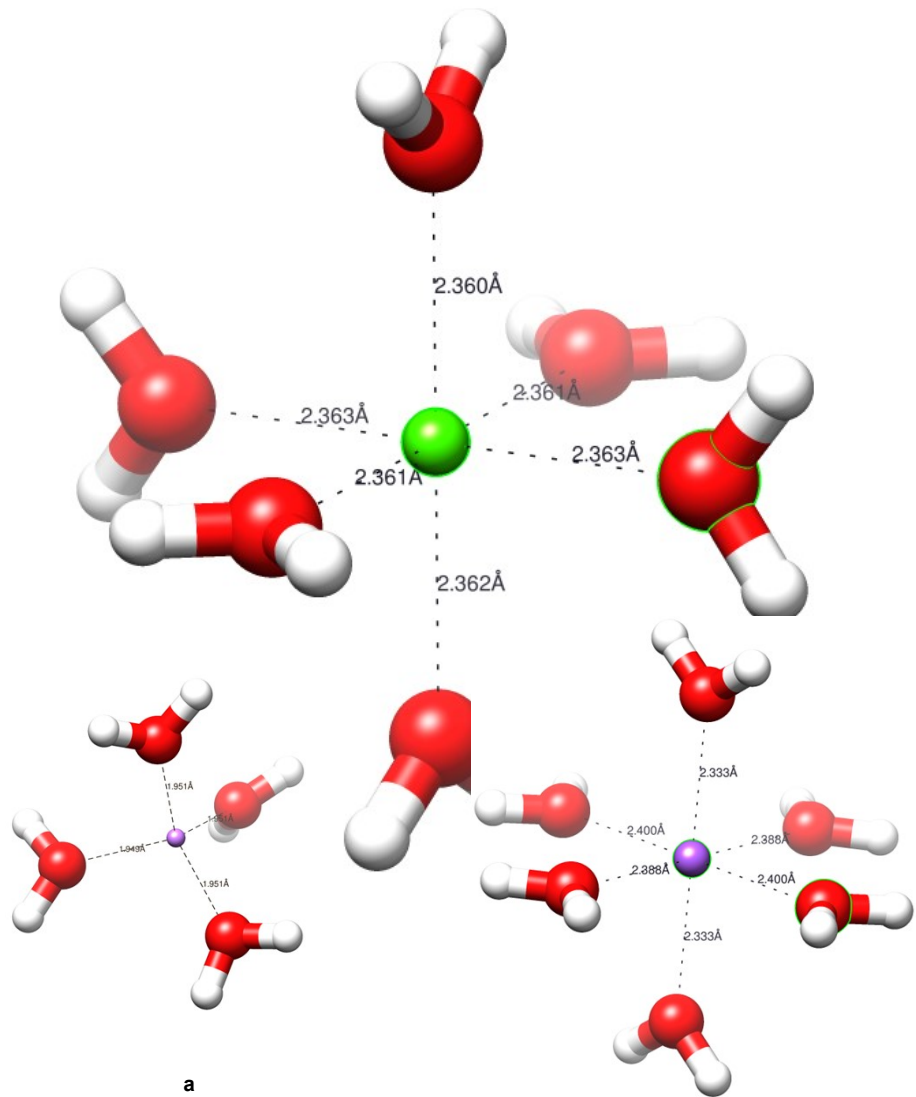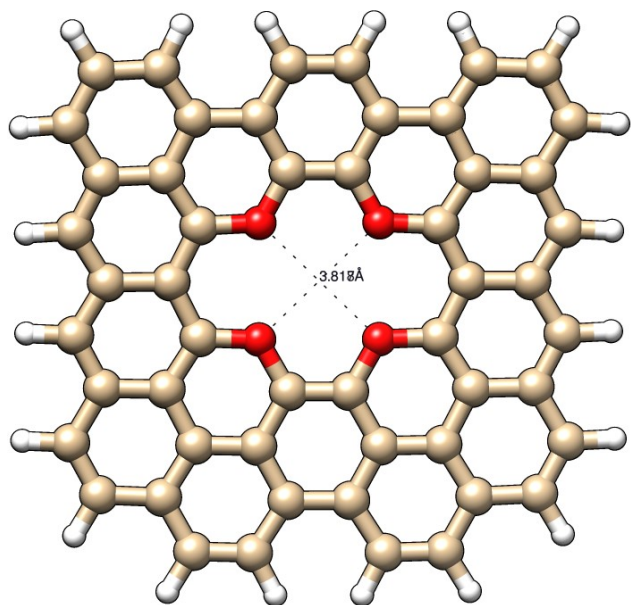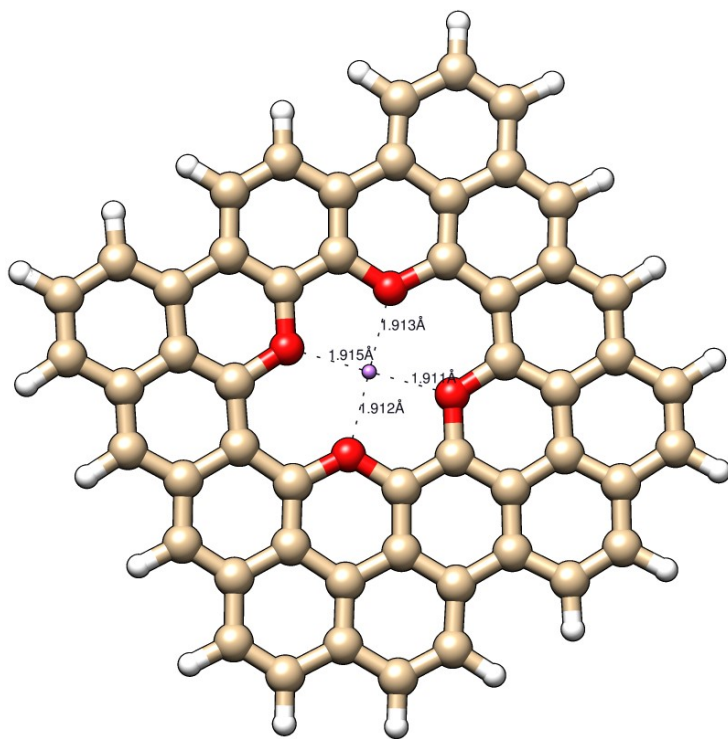
a

b

c

d

e

f
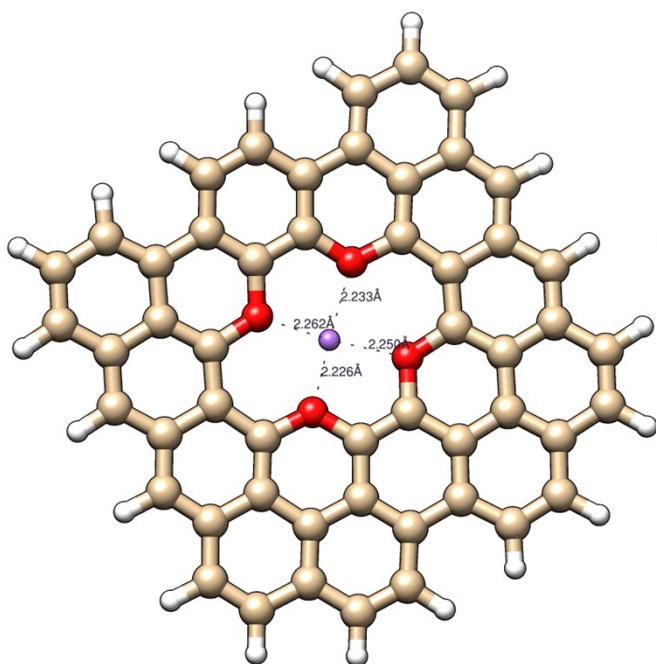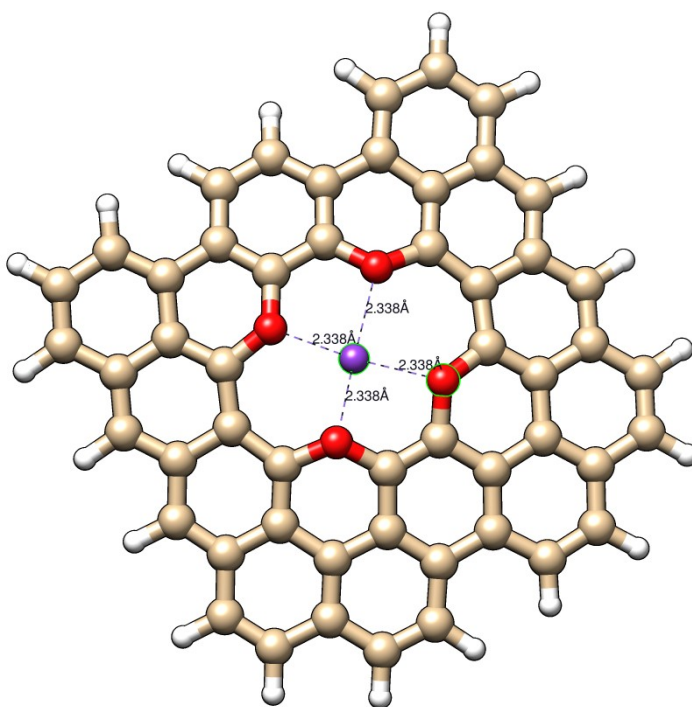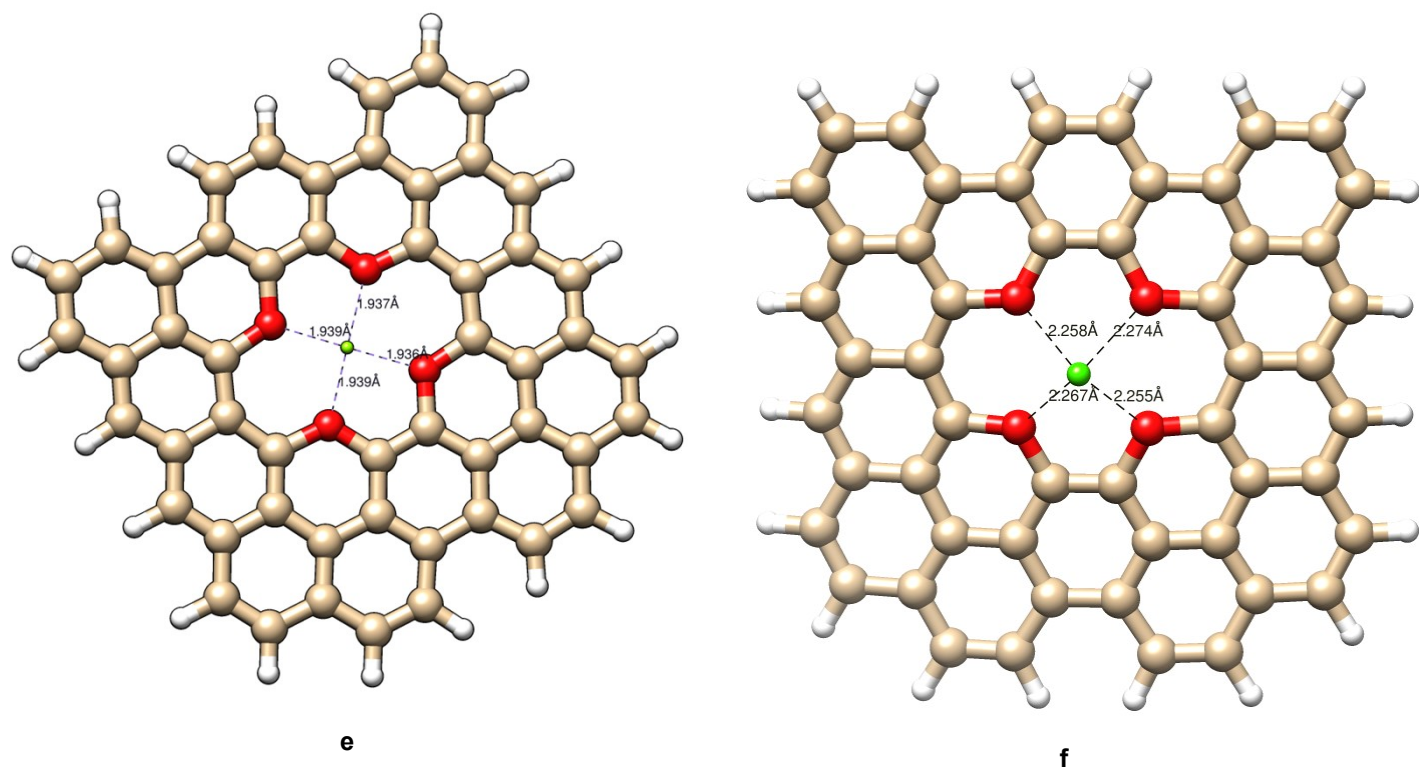
Fig. S2: Optimized structure of hydrated metal ions at the M06-2X/SVP level of theory. (a) [Li-$(H_2O)_6]^+$ (b) [Na-$(H_2O)_6]^+$ (c) [K-$(H_2O)_6]^+$ (d) [Mg-$(H_2O)_6]^{2+}$ and (e) [Ca-$(H_2O)_6]^{2+}$.

a

b

c

d

e

f
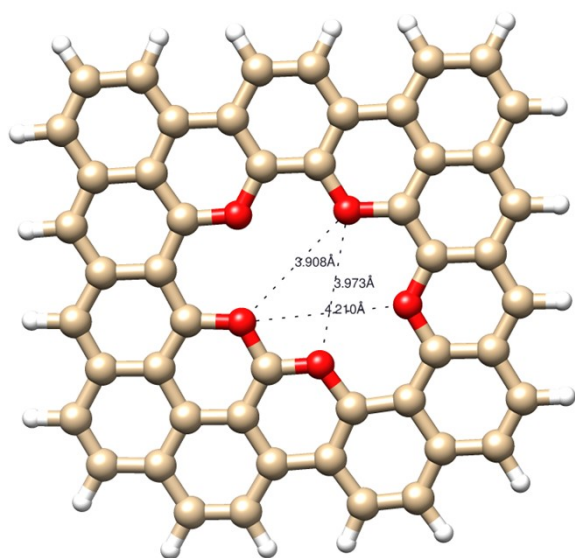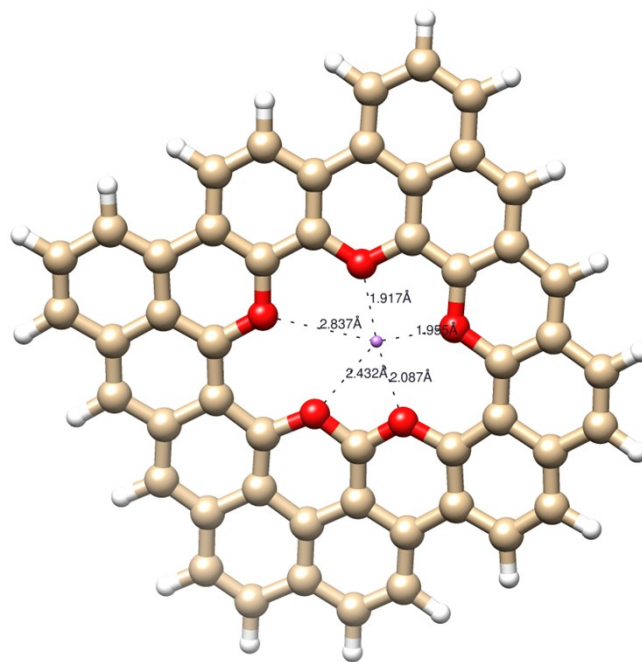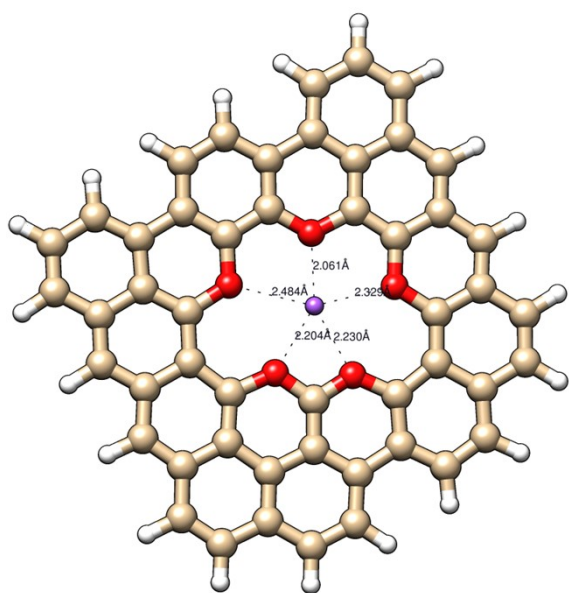
Fig. S3: Optimized structure of hydrated metal ions at the M06-2X/SVP level of theory. (a) [Li-$(H_2O)_6$]$^+$ (b) [Na-$(H_2O)_6$]$^+$ (c) [K-$(H_2O)_6$]$^+$ (d) [Mg-$(H_2O)_6$]$^{2+}$ and (e) [Ca-$(H_2O)_6$]$^{2+}$.

a

b

Fig. S4: Optimized structure of hydrated metal ions at the M06-2X/SVP level of theory. (a) [Li-$(H_2O)_6$]$^+$ (b) [Na-$(H_2O)_6$]$^+$ (c) [K-$(H_2O)_6$]$^+$ (d) [Mg-$(H_2O)_6$]$^{2+}$ and (e) [Ca-$(H_2O)_6$]$^{2+}$.

Distance from mean plane (G-14C4-Na) 1.160Å

Distance from mean plane (G-14C4-K) 1.054Å

Distance from mean plane (G-14C4-Ca) 1.175Å

Distance from mean plane (G-16C5-k) 1.617Å

Distance from mean plane (G-16C5-Ca) 0.852Å
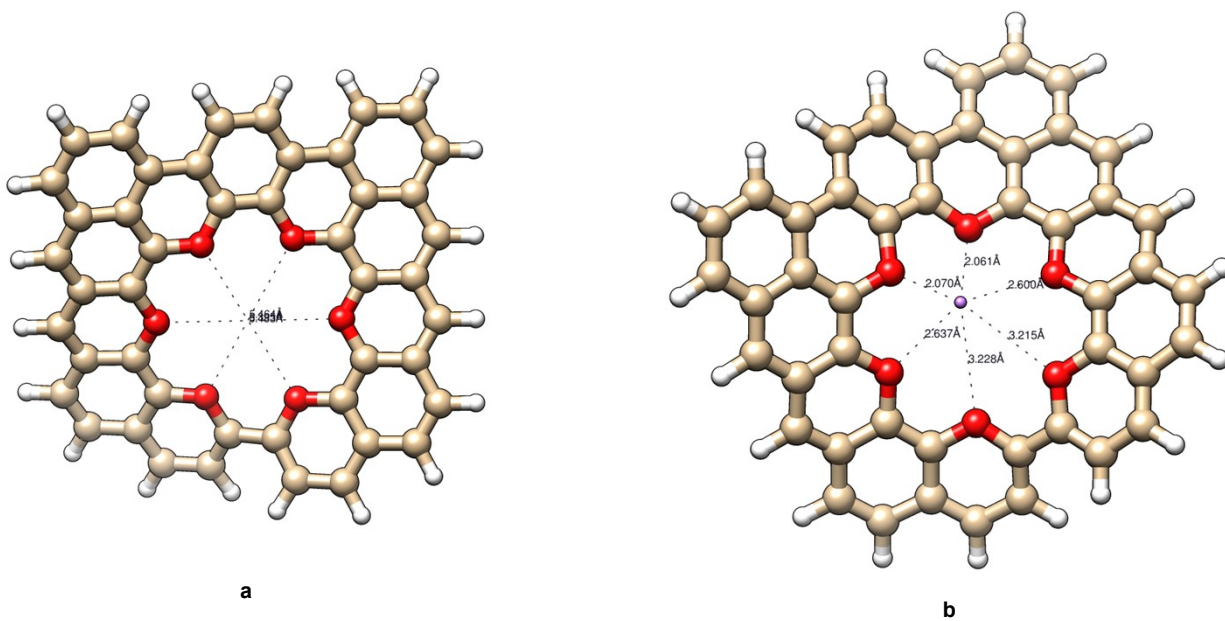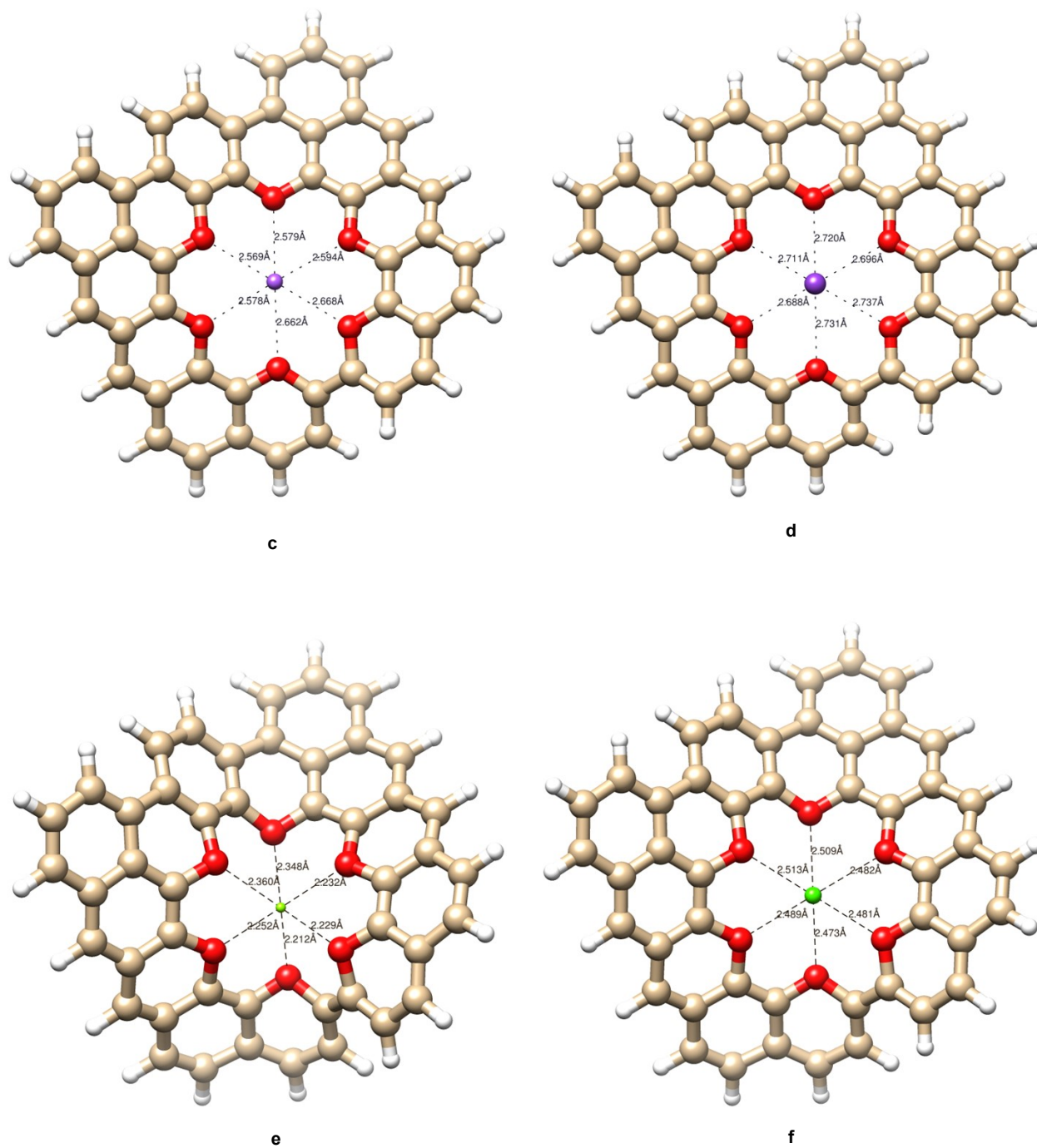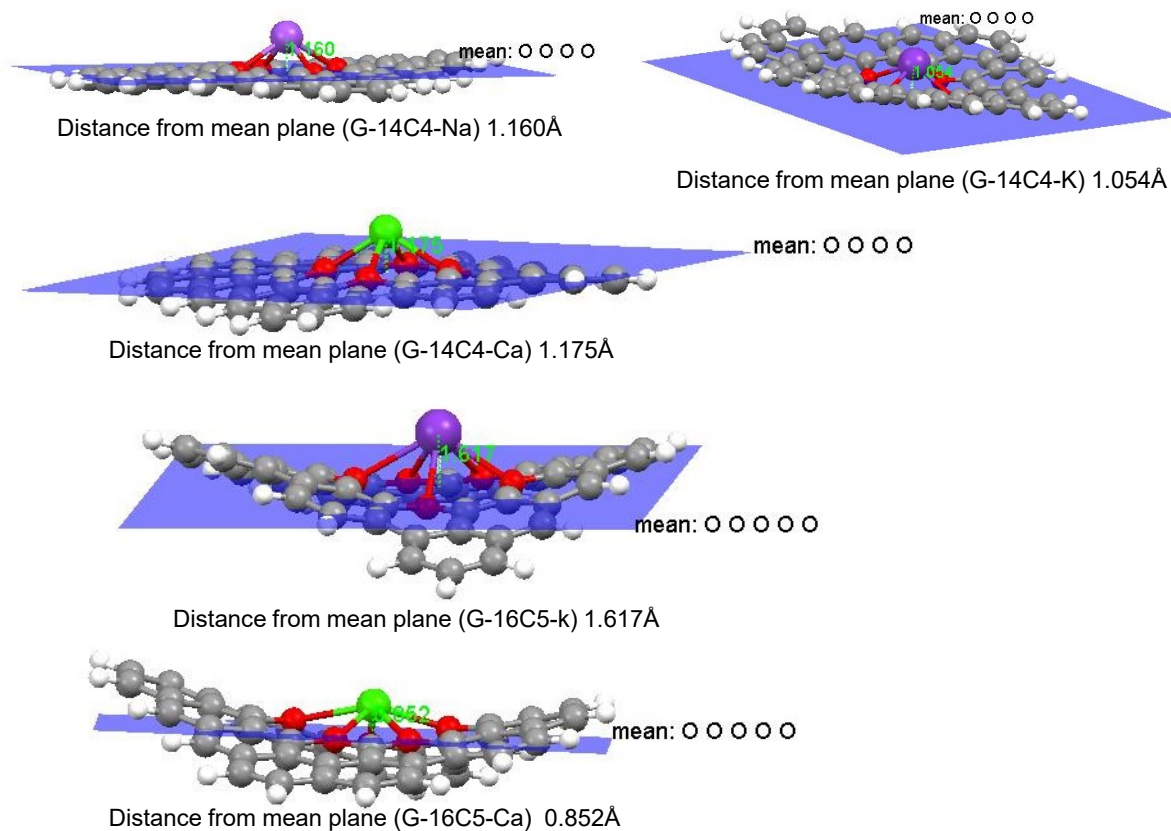
Fig. S5: Calculated distances from mean plane for metal ions which are located above the mean plane of the graphene crown ether pore.

From **Fig. S5,** it can be noticed that Na, K and Ca ions are not encapsulated within the cavity of GO-14C4. They sit above the pore plane. Whereas in the case of GO-16C5, K and Ca ions are not encapsulated within the cavity. This arises due to the larger size of the cations with respect to the respective pore size.

Table S1. Calculated M-O bond distances with hydrated metal ions and encapsulated graphene-crown nanopores at the M06-2x/SVP level of theory in gas phase.

System	M-O bond distances (Å)				
	Li-O	Na-O	K-O	Mg-O	Ca-O
H_2O	1.954	2.373	2.798	2.082	2.361
G-14C4	1.912	2.242	2.338	1.937	2.263
G-16C5	1.917-2.837	2.061-2.484	2.601.2.861	1.959-2.333	2.227-2.433
G-18C6	2.061-3.228	2.569-2.688	2.688-2.737	2.212-2.360	2.473-2.513

From **Table S1,** the bond length of metal ion in hydrated cluster follows the order: LiO<MgO<CaO<NaO<KO. Similar order is followed for G-14C4 except Ca-O which is longer than NaO. In the case of G-16C5, the order of bond length is LiO<MgO<NaO<CaO<KO, whereas for G-18C6, the order is LiO<MgO<CaO<NaO<KO. The M-O bond length is smaller in G-14C4 and G-16C5 than M-O bond length in hydrated metal ion, whereas it is longer in G-18C6 for all the met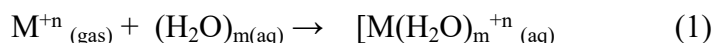al ions except K ion, where it is found to be shorter than corresponding hydrated one which might be indicating of its perfect fitting.

Text S2. Free energy of hydration

The hydration energy was determined by considering the first solvation sphere water molecules (assuming 6 water units) as

$$M^{+n}_{(gas)} + (H_2O)_{m(aq)} \rightarrow [M(H_2O)_m^{+n}]_{(aq)} \qquad (1)$$

The cluster method of Goddard et al [10] was adopted here (optimized structures are shown in **Fig. S1)**. The calculated hydration energy (kcal/mol) of metal ions at the M06-2x/TZVP level of theory.

Table S2. Calculated hydration energy (kcal/mol) of metal ions at the M06-2x/TZVP level of theory using cluster model.

System	Hydration energy		
	DFT (cluster)	DFT (implicit)	Experiment
$[Li-(H_2O)4]^+$	-130.3	-103.6	-122.1
$[Na-(H_2O)6]^+$	-114.0	-90.3	-98.2
$[K-(H_2O)6]^+$	-95.8	-73.1	-80.6
$[Mg-(H_2O)6]^{+2}$	-458.6	-397.2	-455.5

| [Ca-(H₂O)6]⁺² | -389.1 | -292.2 | -380.8 |

The calculated hydration energy using DFT follows the order: $Mg^{+2} > Ca^{+2} > Li^+ > Na^+ > K^+$. The computed results using cluster approach are in good agreement with the reported experimental results compared to implicy model. During complexation with G-crown ether, the metal ion can bind within the cavity either in hydrated or partially hydrated or fuly dehydrted form depending on the value of hydration energy. As per hydration energy is concerned, the dehydration energy is least for K^+ ion and maximum for Mg^{2+} ion. If dehydration energy is the sole criteria, then the
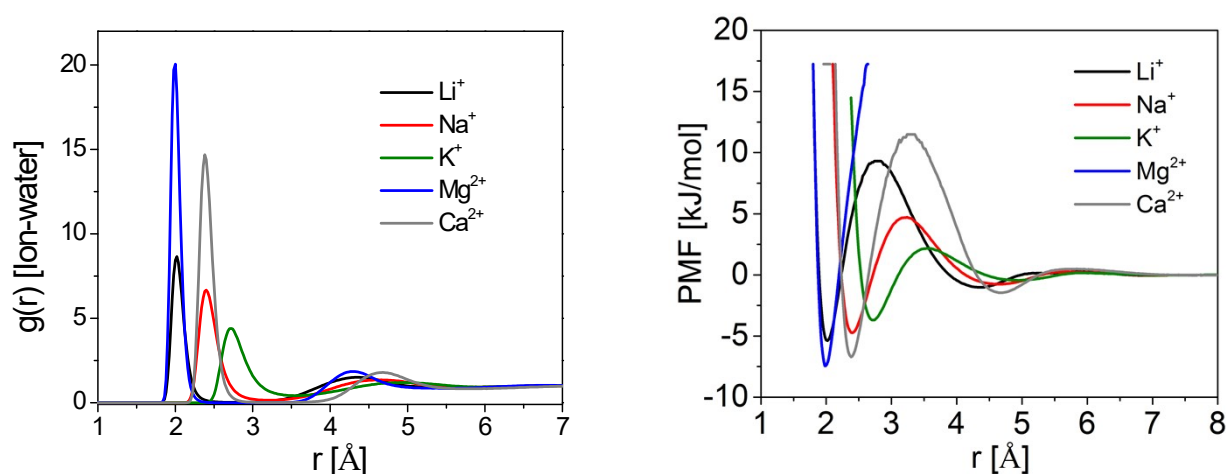
selectvity of the cation will be as follows: $K^+ > Na^+ > K^+ > Ca^{+2} > Mg^{2+}$. Similar obsevation can also be drawn from potntial of mean force (PMF) for bulk hydrated metal ion using MD simulations.

Fig. S7: Calculated RDF and PMF for bulk ion-water system. The free energy required to release water molecule from the first hydration shell follows the order: $Mg^{+2} > Ca^{+2} > Li^+ > Na^+ > K^+$.

Text S3. Free energy of complexation

The free energy of complexation was determined as per the following gas phase and aqeous complexation reaction:

$$[M]^{+n}_{(gp)} + L_{(gp)} \rightarrow [ML]^{+n}_{(gp)} \qquad (2)$$

$$[M(H_2O)_6]^{+n}_{(aq)} + L_{(aq)} \rightarrow [ML]^{+n}_{(aq)} + 6H_2O_{(aq.)} \qquad (3)$$
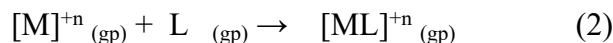
L stands for G-14C4, G-16C6 or G-18C6 grafted graphene crown pores Here "gp" and "aq." Stand for gas phase and aqeous phase respectvely. The free energy of complexation was evaluated as per the standard thermodynamic methods reported elsewhere[11].

Table S3. Calculated free energy of complexation (kcal/mol) for metal ions at the M06-2x/TZVP level of theory in gas phase using bare metal ion.

System	Free energy of complexation (kcal/mol)				
	Li^+	Na^+	K^+	Mg^{+2}	Ca^{+2}
G-14C4	-80.4	-50.9	9.7	-251.8	-180.8
G-16C5	-74.6	-49.8	-39.4	-245.5	-185.5
G-18C6	-78.5	-72.4	-57.9	-251.2	-217.1

From **Table S3**, it is seen that the free energy of complexation increases with increasing cavity size as well as with increasing number of donor atoms only for K^+ and Ca^{+2} ions as one move from G-14C4 to G-16C5 to G-18C6. Whereas for Li^+, Na^+ and Mg^{+2} ions, the free energy is decreased from G-14C4 o G-16C5 but increased as one move from G16C5 to G-18C6. Point to be noted that the free energy of complexation for Li^+ and Mg^{+2} ions with G-18C6 is smaller than that of G-14C4 but for Na+ ion it is higher in G-18C6 than G-14C4. In absence of any solvent (gas phase) the complexation strength for G-14C4, G-16C5 and G-18C6 follows the trend: $Mg^{+2} > Ca^{+2} > Li^+ > Na^+ > K^+$.

Table S4. Calculated free energy of complexation (kcal/mol) for metal ions at the M06-2x/TZVP level of theory in aqueous phase using hydrated metal ion (implicit).

System	Free energy of complexation (kcal/mol)				
	Li^+	Na^+	K^+	Mg^{+2}	Ca^{+2}
G-14C4	-1.7	7.2	57.2	17.4	-13.3
G-16C5	0.5	12.4	2.3	17.7	-16.0
G-18C6	1.8	-3.6	-4.2	41.3	-33.2

From **Table S4**, it is seen that the free energy of complexation in aqueous phase (hydrated metal ions) does not follow similar trend as revealed from the gas phase complexation data (Table **S3**). As one moves from G-14C4 to G-16C5 to G-18C6, the free energy of complexation is seen to be increased for K^+ and Ca^{2+} ion. Whereas for other metal ions, it is decreased except Na^+ ion, where the free energy is increased from G-16C5 to G-18C6. In the case of G-14C4, the complexation strength follows the order: $Ca^{+2} > Li^+ > Na^+ > Mg^{+2} > K^+$, whereas for G-16C5, the order is: $Ca^{+2} > Li^+ > K^+ > Na^+ > Mg^{+2}$. The complexation order with G-18C6 is: $Ca^{+2} > K^+ > Na^+ > Li^+ > Mg^{+2}$. The results indicate that the metal ion selectivity is a complex parameter which depends on the hydration energy of the metal ion, size and shape of the host cavity and the number of donor atoms within the cavity. For large cavity, the selectivity is purely dictated by dehydration energy of the metal ions. Whereas for small cavity, the selectivity is dictated by dehydration energy of the metal ions as well as size and shape of the host cavity. The selectivity of Ca^{2+} ion is always high due to underestimation of hydration energy of Ca^{2+} ion using implicit hydration model (**Table S2**).

Table S5. Calculated free energy of complexation (kcal/mol) for metal ions at the M06-2x/TZVP level of theory in aqueous phase using hydrated metal ion (explicit).

System	Free energy of complexation (kcal/mol)				
	Li^+	Na^+	K^+	Mg^{+2}	Ca^{+2}
G-14C4	-13.8	-27.8	15.1	24.3	28.7
G-16C5	-5.0	-15.9	-39.6	24.6	26.1
G-18C6	-3.7	-17.9	-46.2	48.2	8.8

Text S4. Effect of Cation-Π interaction

DFT study: M06-2x/TZVP level of calculations using Turbomole program

The cation-Π interaction energy for graphene-cation-water was determined using the method of G. Shi et al.[12]. The cation-pi interaction energy for graphene-cation-water (only two water molecules were considered as only two water molecules were observed in the direct coordination of adsorbed Na ion in the crown pore of graphene) was seen to be higher (-31.1-(-4.3) = -26.8 kcal/mol) than that of cation-pi-crown-dipole water interaction energy (-49.2- (-45.5) = -3.7 kcal/mol). The DFT data in **Table S6** shows that in presence of crown dipole (like in present membrane system) the cation-pi interaction is dominated by the crown-dipole-cation interaction rather than cation-pi interaction. Therefore, it can be expected that cation-pi interaction would not affect the reported MD data and trends, where MD simulations were carried without considering cation-pi interactions. It is also worthwhile to mention here that earlier Jian Liu et al. (Phys. Rev. Lett. 2015, 115, 164502) reported that functionalization of CNT weakens the cation-pi interaction. In the present study, the functionalization of graphene has been done by creating crown ether pore within the graphene surface which also reduce the exposed surface of the graphene.

Table S6. Energy required for different complexation reactions from DFT simulations

Complexation reaction	Energy (kcal/mol)
Graphene + Na-$(H_2O)_2$ = Graphene-Na-$(H_2O)_2$	-31.1
Graphene + $(H_2O)_2$ = Graphene-$(H_2O)_2$	-4.3
G-16C5 + Na-$(H_2O)_2$ = G-16C5-Na-$(H_2O)_2$	-49.2
G-16C5 + $(H_2O)_2$ = G-16C5 -$(H_2O)_2$	-45.5

Ab-initio Study

A simulation box (20×20×20 Å^3) containing one graphene-16C5 membrane, 3 cations (one Na$^+$, Li$^+$ and K$^+$ each), 3 chloride ions and 64 water molecules was simulated in VASP for 20 ps at T =400K using PBE functional and PAW potential[13, 14]. The generated data was compared with MD results as reported here.

Comparison of Classical MD (CMD) and Ab-initio MD (AIMD) results
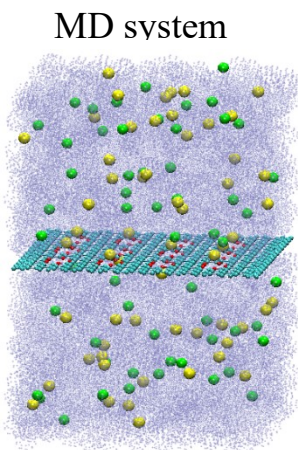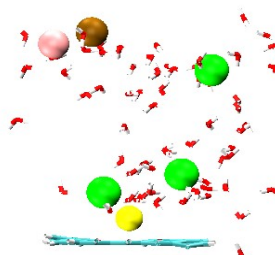
MD system   Ab-initio-MD system

Fig. S8: Snapshot of simulated system using CMD and AIMD

i) Selectivity of cation –

Both the studies show preferential adsorption of Na^+ ions over other cation for graphene-16C5 membrane

ii) Position of adsorbed Na^+ ions:

From AIMD simulation, the vertical (z) distance of Na^+ from graphene was noted to be 2.1 Å, which is as per peak intensity obtained from MD simulation. Distance of Na^+ from crown ether oxygen was 2.9 Å.
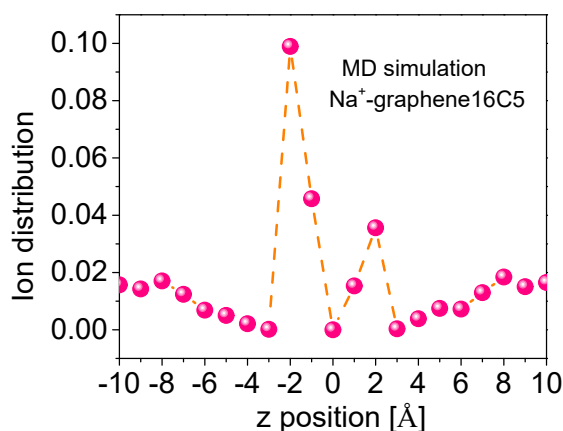

Fig. S9: Na^+ ion distribution profile for graphene-16C5 membrane aqueous system from MD simulations

iii) Hydration number of adsorbed Na^+ ions:

Secondly, the adsorbed Na^+ ion was seen to be partially dehydrated. Total hydration number of adsorbed Na^+ was 2 in AIMD simulation, which is also in agreement with MD observation where hydration number of Na^+ was noted in between 2 to 3 with average hydration number of ~2.5
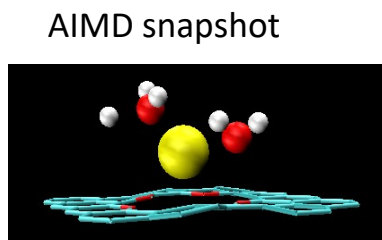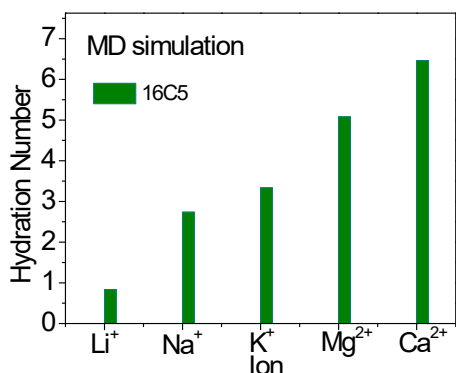
Fig. S10: Hydration number of adsorbed Na+ ions from CMD and AIMD simulation

iv) Ion-water structuring for adsorbed Na$^+$ ions:

From AIMD, Na-O$_{water}$ peak noted at 2.3 Å, which is very close to MD estimated value of 2.45 Å.
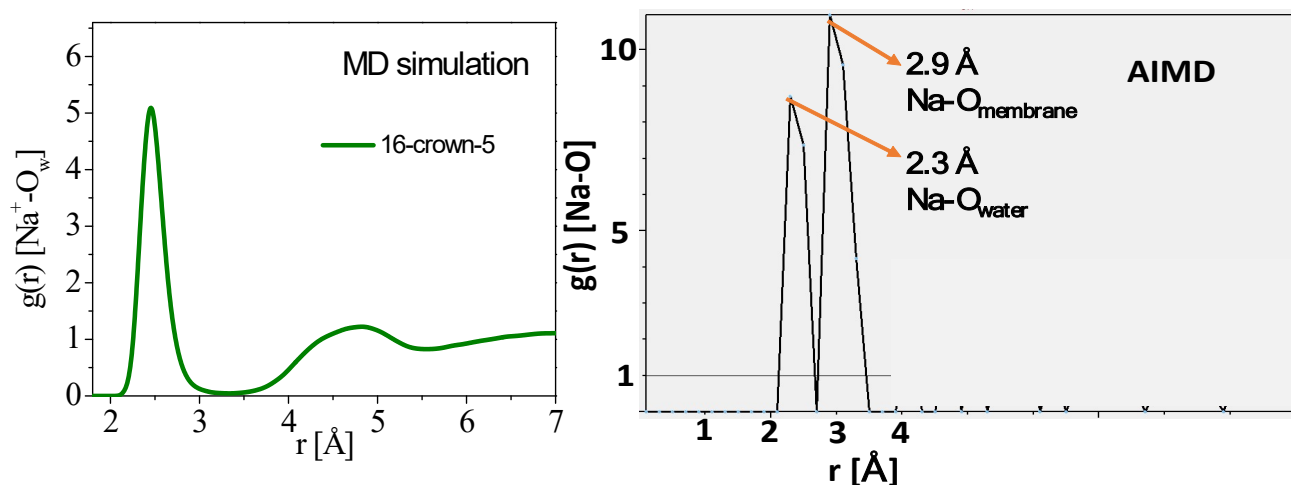

Fig. S11: RDF profile for Na-O$_{water}$ from CMD simulations and Na-O$_{water}$ and Na-O$_{membrane}$ from AIMD simulations (for adsorbed Na$^+$ ion)

Hereby, the presented similarity of AIMD data and MD results indicate that the cation-pi interaction would not affect the reported MD data and trends, even-when MD simulations were carried without considering cation-pi interactions.

Text S5. Impact of pressure on ion capacity of graphene-crown membrane

To evaluate the impact of pressure on ion adsorption capacity of crown ether graphene membranes, we performed adsorption studies of Na$^+$ and Li$^+$ ions within graphene-14C4 pores using NPT ensemble, where pressure of the system was varied to be 1 bar, 10 bar, 20 bar and 50 bar (from both ±z direction such that membrane feels equal pressure from top and bottom) keeping system temperature constant as 300 K. The system dynamics was performed for 100 ns and the data

generated in last 50 ns was used for analysis of adsorption capacity. The respective adsorption data is shown in enclosed **Figure S12**, which represents the increasing ion adsorption with increasing pressure for both the Li$^+$ as well as Na$^+$ ions. However, for all the considered pressure, the adsorption capacity of Na$^+$ ions within graphene-14C4 membrane was much higher than Li$^+$ ions. The observations show that though increase in pressure leads to minor increase in ion adsorption of graphene-crown membrane, nevertheless, the trend for preferential adsorption of particular cation with considered membrane remains unaffected.
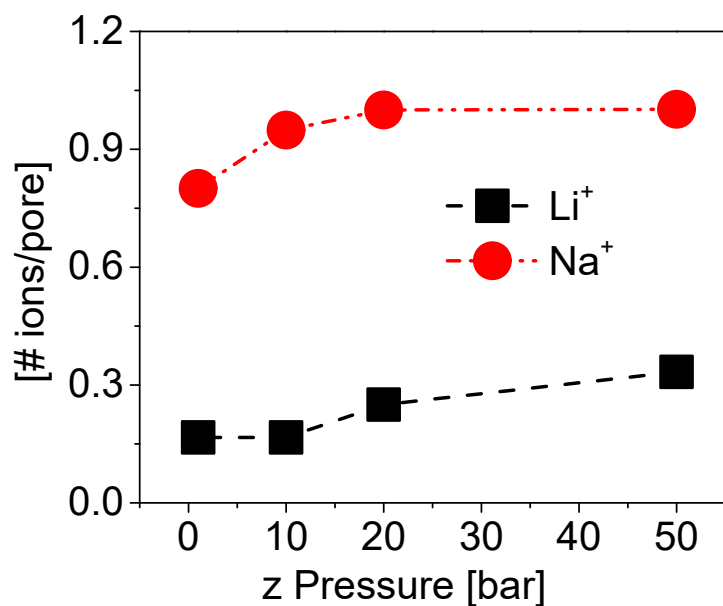

Fig. S12: Impact of pressure on ion adsorption capacity of graphene-14C4 membrane for Li$^+$ and Na$^+$ cations.

Text S6. Pressure fluctuation in MD simulations

The pressure fluctuations were observed to be very high in MD simulations of aqueous solutions as shown in **Figure S13**. The high pressure fluctuations in pressure for present system is expected from the nearly incompressible nature of water.

The standard deviation of pressure can be estimated using the formulation –

$$\sigma_P = \sqrt{\frac{\rho c^2 kT}{V}}$$

Taking the values for water at standard conditions $\rho=997$ kg/m^3, c=1500 m/s,T=298.15 K, and box volume of 96 nm^3, the pressure fluctuation was estimated to be : 983.5 bar
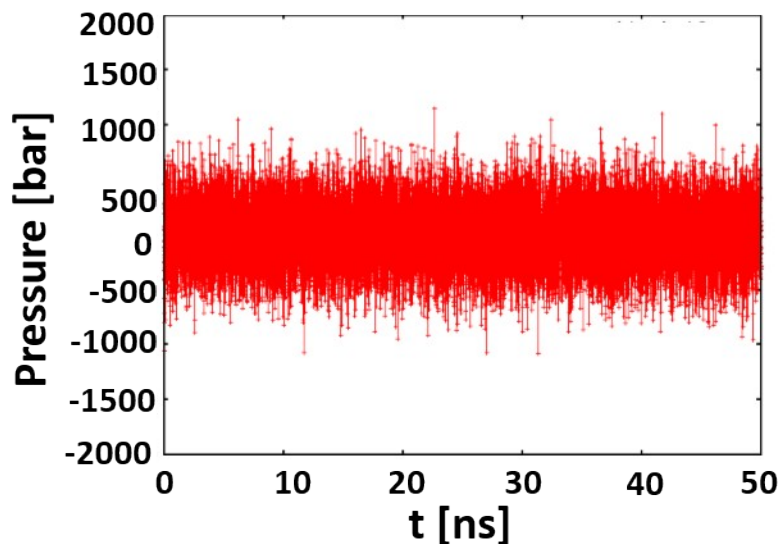Therefore, the obtained fluctuation of $\pm$ 1000bar is as per expectation.

Fig. S13: Pressure fluctuation in MD simulation systems (graph shown for NaCl-water-graphen14C4 system)

References

(1) TURBOMOLE, University of Karlsruhe, Germany, 1988. Ahlrichs, R.; Bar, M.; Haser, M.; Horn. H.; Kolmel, C. Chem. Phys. Lett. 1989,162, 165−169.
(2) Zhao, Y.; Truhlar, D.G. Density Functionals with Broad Applicability in Chemistry, Acc. Chem. Res. 2004, 37, 157.
(3) A. Schäfer, H. Horn and R. Ahlrichs; J. Chem. Phys. 97, 2571 (1992).

(4) A. Schäfer, C. Huber and R. Ahlrichs; J. Chem. Phys. 100, 5829 (1994).

(5) Klamt, A. Conductor-like screening model for real solvents: A new approach to the quantitative calculation of solvation phenomena. J. Phys. Chem. 1995, 99, 2224-2235.

(6) Pettersen, E.F.; Goddard, T.D.; Huang, C.C.; Couch, G.S.; Greenblatt, D.M.; Meng, E.C.; Ferrin, T.E. J. Comp. Chem. 2004, 25, 1605-12.

(7)McQuarrie, D.A. Statistical Mechanisc, Harper & Row, New York, 1976.

(8) Velde, G. te.; Bickelhaupt, F.M.; Baerends, E.J.; Fonseca Guerra, C. ; van Gisbergen, S.J.A.; Snijders, G.J.; Ziegler, T. Chemistry with ADF, J. Comp. Chem. 2001, 22, 931.

(9) ADF2017, SCM, Theoretical Chemistry, Vrije Universiteit, Amsterdam, The Netherlands, http://www.scm.com.

(10) Bryantsev, V.S.; Diallo, M.S.; Goddard III, W.A. J. Phys. Chem. B. 2008, 112, 9709.

(11) De S, Ali SM, Ali A, Gaikar VG (2009) Phys Chem Chem Phys 11: 8285.

(12) Guosheng Shi, Jian Liu, Chunlei Wang, Bo Song, Yusong Tu, Jun Hu and Haiping Fang; Ion Enrichment on the Hydrophobic Carbon-based Surface in Aqueous Salt Solutions due to Cation-p Interactions *Scientific Reports* (2013) **3**: 3436

13) Perdew J P, Burke K and Ernzerhof M; Generalized Gradient Approximation Made Simple *Phys. Rev. Lett*. (1996) **77**, 3865

14) Kresse G and Hafner J; Ab initio molecular dynamics for open-shell transition metals *Phys. Rev.* B (1993) **48** 13115